Proceedings of the Seventh International Conference on
Railway Technology: Research, Development and Maintenance
Edited by: J. Pombo
Civil-Comp Conferences, Volume 15, Paper 18.14
Civil-Comp Press, Edinburgh, United Kingdom, 2026
ISSN: 2753-3239, doi: 10.4203/ccc.15.18.14

Asymmetric Wheel–Rail Interaction and Derailment Risk in Curved Railway Tracks with Transition Geometry Considering PSD-Based Track Irregularities

P. Gorai, S. K. Saha and R. K. K

Depertment of Mechanical Engineering, Indian Institute of Technology Delhi, New Delhi, India

Abstract

This study investigates asymmetric wheel–rail interaction and derailment risk in curved railway tracks incorporating transition geometry and measured track irregularities. An integrated multibody dynamic model based on the European Railway Research Institute (ERRI) formulation is implemented in VI-Rail to simulate realistic wheel–rail contact behaviour, suspension dynamics, and vehicle–track interaction under varying curve radii, vehicle speeds, and irregularity conditions. The derailment coefficient lateral-to-vertical force ratio (L/V) exhibits a progressive increase within the transition region owing to the gradual introduction of curvature and cant, reaching its peak at the onset of the circular track. Thereafter, the force response tends toward a quasi-steady oscillatory behaviour in the curved section, suggesting a stabilized wheel–rail interaction under constant curvature conditions. A non-monotonic speed dependence is observed, with L/V decreasing from approximately 0.58 at 40 km/h to 0.49 at 100–120 km/h, followed by an increase to nearly 0.55 at 140 km/h. Curve radius strongly influences derailment behaviour, where sharp curves ($R = 250\,\mathrm{m}$) produce significantly higher L/V values, while larger radii ($R = 500\,\mathrm{m}$) maintain comparatively stable operation. Under severe operating conditions, pronounced L/V spikes and near-zero vertical wheel loads indicate elevated derailment susceptibility and intermittent wheel–rail contact loss. The findings highlight the coupled influence of speed, track geometry, and PSD-based track irregularities on vehicle stability, emphasizing the importance of asymmetric wheel–rail interaction in derailment assessment and safer railway track design.

Keywords: wheel–rail interaction, curved track dynamics, stochastic track irregularities, transition curves, derailment risk, multibody dynamics

1 Introduction

The interaction between railway vehicles and track significantly influences running stability, ride quality, component wear, and overall operational safety. This interaction becomes more critical with increasing train speeds and axle loads, especially in curved track sections where centrifugal effects, cant variation, and track geometry considerably affect wheel–rail contact conditions. Consequently, wheel–rail forces become highly dynamic and may exhibit asymmetric behaviour, which can adversely affect vehicle stability. Under such operating conditions, excessive lateral forces and wheel unloading may develop, increasing the likelihood of instability and derailment [2–5, 18, 20].

Curved tracks are especially susceptible to asymmetric wheel–rail interaction due to unequal loading between the inner and outer rails. This asymmetry arises from centrifugal forces and cant imbalance, leading to variations in contact forces, creepages, and wheel unloading [5, 9]. To improve ride comfort and reduce abrupt changes in curvature, transition curves are introduced between tangent and circular track sections. However, transition regions also create complex transient dynamic conditions because curvature and cant vary continuously, often making these sections more sensitive to instability [13, 15, 18].

Accurate prediction of wheel–rail interaction requires robust contact modelling and validated multibody dynamic formulations. Classical rolling contact theory developed by Kalker [1] forms the basis for creep force estimation, while the nonlinear contact formulations proposed by Polach [4, 5] provide improved representation of adhesion-limited wheel–rail behaviour. In addition, multibody railway vehicle models have been widely employed to capture suspension dynamics, wheelset motion, and contact nonlinearity under realistic operating conditions [7, 14, 19]. Benchmark vehicle formulations such as the ERRI model have therefore become important tools for railway dynamic analysis [21].

Apart from geometric effects, railway tracks contain unavoidable irregularities due to wear, maintenance limitations, and construction tolerances. These irregularities act as stochastic excitation sources and significantly affect vehicle dynamic response [6, 11, 22]. Several studies have demonstrated that track irregularities can amplify wheel–rail contact forces and degrade vehicle stability, particularly in curved track conditions

[9, 10, 15, 17]. Power spectral density (PSD)-based representation is commonly used to model realistic irregularity profiles while preserving the statistical characteristics of measured track data [6].

Several studies have examined curved track dynamics, vehicle–track interaction, and derailment behaviour under different operating conditions [10, 12, 17, 23]. While the influence of track irregularities on derailment response has been investigated, the combined effect of transition geometry and PSD-based track irregularities on asymmetric wheel–rail interaction has received comparatively less attention. In particular, the variation of wheel unloading and the lateral-to-vertical force ratio within transition regions, where curvature and cant evolve simultaneously, is not yet fully understood. This limitation motivates the need for a detailed investigation of derailment behaviour under realistic irregular track conditions.

The present study investigates asymmetric wheel–rail interaction and derailment risk in curved tracks with transition geometry under stochastic track irregularities using a validated multibody dynamic framework. A benchmark ERRI-based railway vehicle model implemented in VI-Rail is adopted to simulate realistic wheel–rail contact behaviour. PSD-based track irregularities are incorporated to represent realistic excitation conditions, and the effects of speed, curve radius, and irregularity levels on wheel–rail forces, asymmetric loading, and derailment indicators are systematically examined.

2 Methodology

This section presents the methodology adopted to investigate the dynamic response of the railway vehicle under curved track conditions. The vehicle–track interaction model, track geometry, and PSD-based track irregularities considered in the simulations are first described, followed by the parametric framework used to evaluate the influence of operating and track conditions on wheel–rail interaction behaviour.

2.1 Vehicle–Track Dynamic Model

A multibody dynamic model of the railway vehicle–track system is employed to investigate wheel–rail interaction under curved track conditions. The simulations are carried out using the commercial software VI-Rail, which incorporates a validated nonlinear multibody formulation for railway vehicle dynamics. The modelling framework enables realistic representation of vehicle response under varying operating conditions, including the effects of wheel–rail contact, suspension dynamics, and track geometry.

The railway vehicle is represented as an interconnected system of rigid bodies comprising the carbody, bogies, and wheelsets, linked through primary and secondary suspension elements. The multibody formulation accounts for the coupled dynamic interaction between the vehicle and track, allowing realistic prediction of wheel–rail forces, load transfer, and vehicle stability in curved track environments.

The vehicle model adopted in the present study is based on a benchmark railway vehicle configuration implemented within the VI-Rail environment. The model incorporates wheelset guidance, suspension characteristics, and wheel–rail contact interactions required for evaluating derailment-related responses under curved track conditions with transition geometry and PSD-based irregularities. A schematic representation of the vehicle model is shown in Fig. 1.

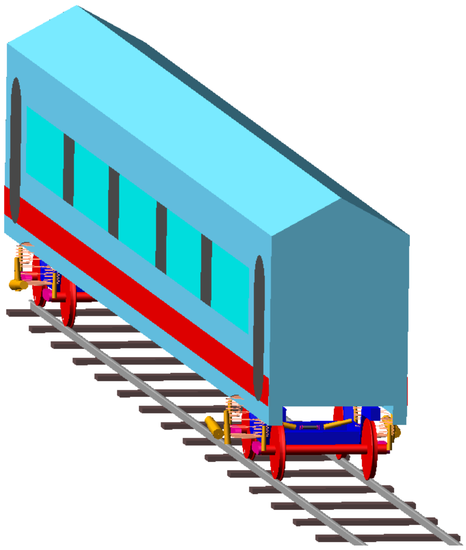

Figure 1: Vehicle Model

2.2 Wheel–Rail Contact Modelling

The wheel–rail interaction is modeled using a nonlinear contact formulation implemented through a standardized contact configuration file (CCF) within the VI-Rail framework. A generalized wheel–rail contact model (WRGEN) is adopted, ensuring consistent contact representation along the entire track length under a uniform configuration. The normal contact force is evaluated based on Hertzian contact theory [1], with a small damping ratio (0.001) incorporated to account for energy dissipation during contact deformation.

The tangential creep forces are computed using Kalker's simplified theory via the FASTSIM algorithm [1], which provides an efficient nonlinear approximation of rolling contact behavior. The creep force formulation is scaled using a Kalker factor of unity, while constant friction coefficients $\mu = 0.4$ are assumed in both longitudinal and lateral directions to maintain numerical stability and computational efficiency. The total contact force is decomposed into normal and tangential components, which together govern the dynamic stability and guidance of the wheelset.

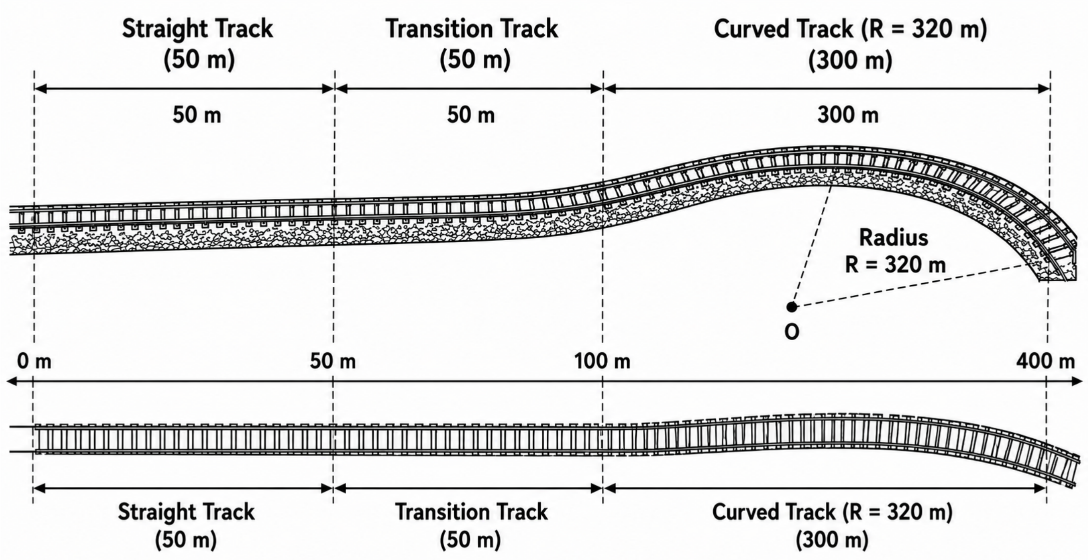

Figure 2: Schematic Diagram of Track

2.3 Track Modelling

The track is modelled analytically within the VI-Rail environment with a total length of 400 m, consisting of a straight segment, a transition region, and a circular curve shown in Fig.2. The standard gauge of 1.435 m is adopted, and measured track irregularities are included to represent realistic operating conditions.

2.3.1 Horizontal Geometry

The curvature $\kappa(s)$ of the track is defined as a piecewise function:

$$\kappa(s) = \begin{cases} 0, & 0 \leq s < 50 \\ \frac{s-50}{50R}, & 50 \leq s < 100 \\ \frac{1}{R}, & 100 \leq s \leq 400 \end{cases} \tag{1}$$

where s is the longitudinal coordinate along the track and $R = 320$ m is the radius of the circular curve. The transition region ensures a gradual increase in curvature.

2.3.2 Cant (Superelevation)

The cant angle $\phi(s)$ is introduced progressively along the transition zone and is defined as:

$$\phi(s) = \begin{cases} 0, & 0 \leq s < 50 \\ \phi_{\max}\frac{s-50}{50}, & 50 \leq s < 100 \\ \phi_{\max}, & 100 \leq s \leq 400 \end{cases} \tag{2}$$

where $\phi_{\max} = 0.1$ rad is the maximum cant angle. This variation results in asymmetric loading between the inner and outer rails.

2.3.3 Track Irregularities

Measured PSD-based track irregularities are incorporated in the VI-Rail model to simulate realistic excitation of the vehicle–track system. Measured PSD data are used to generate lateral and vertical irregularities for both rails, while a scaling factor is employed to investigate the influence of different track quality conditions, ranging from smooth to degraded states.

2.4 Simulation Matrix

A structured simulation matrix is adopted to systematically investigate the influence of key parameters on wheel–rail interaction and derailment risk. The simulations are categorized into four sets.

Table 1: Simulation matrix used for the parametric investigation

Study Type	**Parameter**	**Simulation Cases**	**Fixed Case**
Speed Sensitivity	Train speed	40, 60, 80, 100, 120, and 140 km/h	Baseline geometry with nominal PSD
Track Irregularity	Scaling factor of PSD	No irregularity, $0.5\times$, $1.0\times$, and $1.5\times$ PSD	100 km/h
Curve Radius	Curve radius	250, 320 , and 500 m	100 km/h
Critical Operating Conditions	Combined parameters	Radius = 250, 320, and 500 m with $1.0\times$ and $1.5\times$ PSD	140 km/h

First, a speed variation study is conducted under fixed track conditions to identify critical operating speeds. Second, the influence of track irregularities is examined by varying the PSD scaling factor, representing different levels of track quality ranging from smooth to degraded conditions. Third, the effect of curve radius is analysed to evaluate the influence of track geometry on vehicle stability. Finally, critical operating scenarios are investigated by combining high speeds with severe track conditions, including increased irregularity levels and smaller curve radii.

The analysis focuses on asymmetric wheel–rail interaction, characterized by unequal force distribution between the left and right wheels, particularly in curved track sections. Derailment risk is evaluated using the lateral-to-vertical force ratio (L/V).

3 Results and Discussion

This section presents the simulation results obtained from the vehicle–track dynamic analysis. The effects of key parameters, including vehicle speed, track geometry, and irregularity conditions, are systematically investigated to evaluate their influence on wheel–rail interaction and dynamic response characteristics.

3.1 Effect of Speed under fixed Parameter

The discussion focuses on the front bogie response, as it is the first to encounter track irregularities and therefore provides a better representation of wheel–rail interaction behaviour. The variation of lateral force under fixed parameter conditions is shown in Fig. 3. It can be observed that the lateral force response is strongly influenced by vehicle speed. As the speed increases from 40 km/h to 140 km/h, both the magnitude and oscillatory nature of the lateral force increase noticeably. A transient response is observed in the transition section(approximately 50–100 m), after which the response settles into a quasi-steady oscillatory pattern in the circular section.

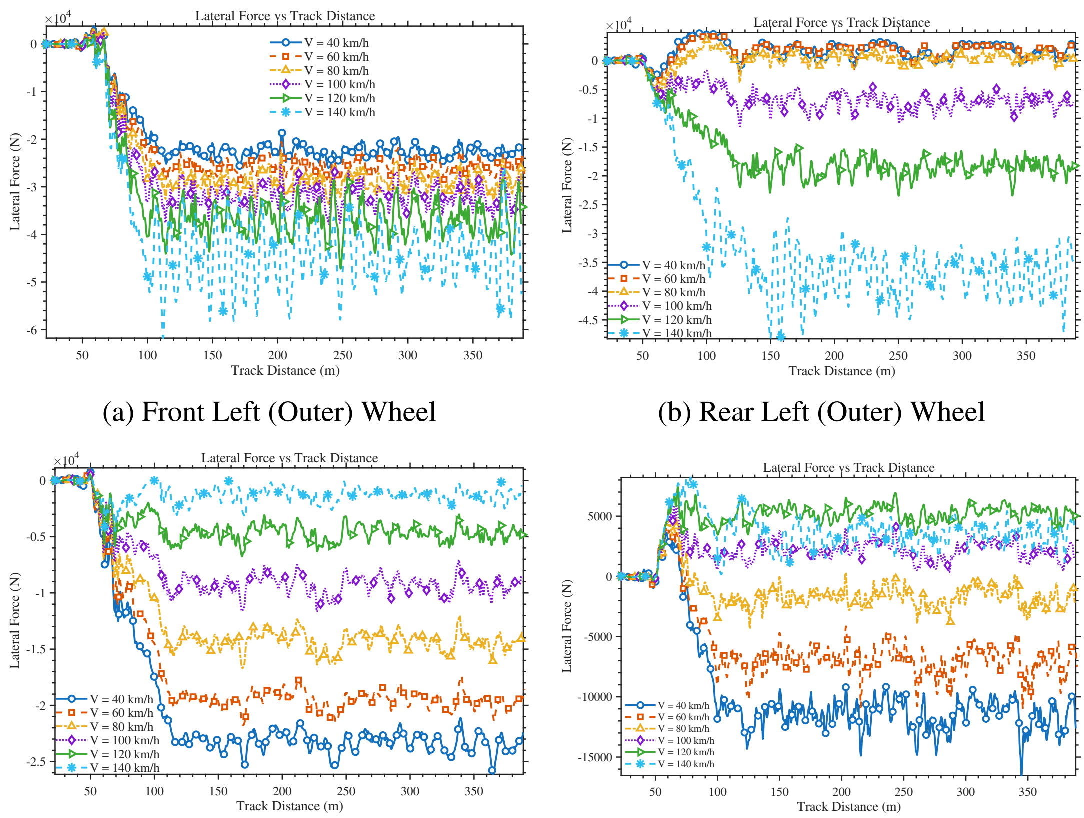

(a) Front Left (Outer) Wheel

(b) Rear Left (Outer) Wheel

(c) Front Right (Inner) Wheel

(d) Rear Right (Inner) Wheel

Figure 3: Lateral force variation of left and right wheels along track distance

Notably, the Rear wheelset (Left and Right wheels) also demonstrates higher sensitivity to speed, with large force fluctuations at higher velocities, indicating potential dynamic instability. The observed asymmetry between left and right wheels highlights the influence of track curvature and non-uniform wheel–rail interaction.

At 140 km/h, the vehicle exhibits high-amplitude oscillations and irregular force variations, suggesting proximity to critical speed conditions and an increased risk of derailment.

The vertical wheel–rail contact force also exhibits a strong dependence on vehicle speed under fixed parameter conditions, as shown in Fig. 4. As speed increases, a significant redistribution of load occurs, with left wheels experiencing increased vertical forces while right wheels undergo substantial unloading. This behavior is primarily attributed to centrifugal effects and vehicle roll dynamics in curved track conditions.

A pronounced transient response is again observed within the initial 100 m, followed by a steady oscillatory pattern. Notably, the right wheels exhibit a sharp reduction in vertical force at higher speeds (120–140 km/h), with values approaching critically low levels. Such unloading significantly increases the risk of derailment, as the lateral-to-vertical force ratio (L/V) becomes large.

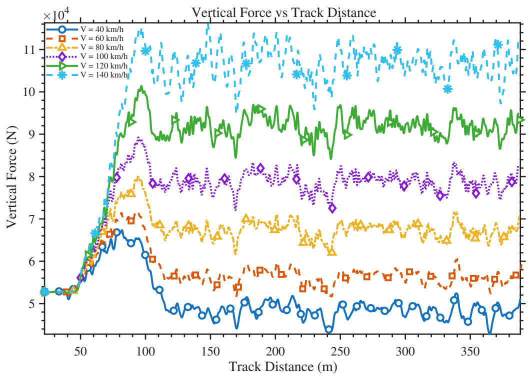

(a) Front Left(Outer) Wheel

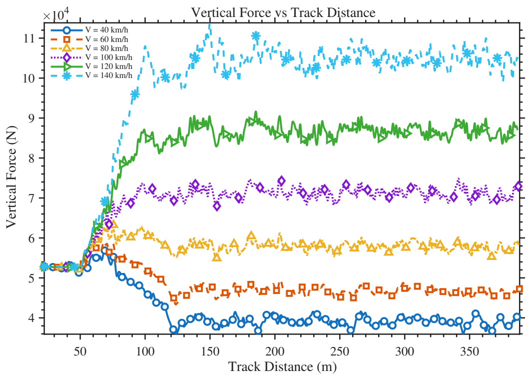

(b) Rear Left(Outer) Wheel

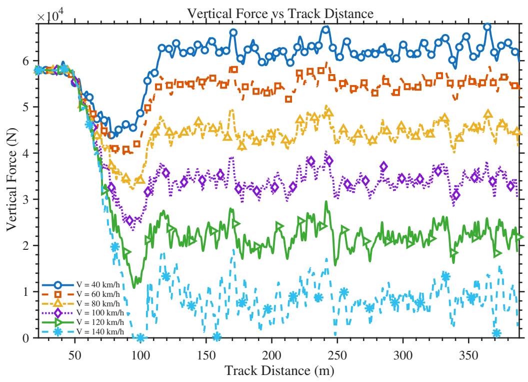

(c) Front Right(Inner) Wheel

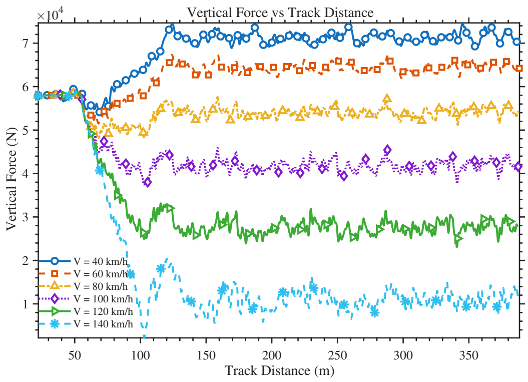

(d) Rear Right(Inner) Wheel

Figure 4: Vertical force variation of left and right wheels along track distance

Overall, the results indicate that at higher speeds, particularly around 140 km/h, the system approaches unsafe operating conditions due to the combined effects of increased lateral forces and reduced vertical contact forces

3.2 Effect of Speed on L/V Ratio

The variation of the derailment coefficient (L/V ratio) with vehicle speed for the front and rear wheelsets is presented in Figures 5 and 6. A consistent trend is observed in both cases, wherein the L/Vratio initially decreases with increasing speed, reaching a minimum around 100–120 km/h, beyond which it increases again at higher speeds.

At lower speeds (e.g., 40 km/h), relatively higher L/V values are observed. This behaviour can be attributed to the increased influence of track irregularities, which induce localized fluctuations in lateral and vertical forces. Due to lower inertial effects, the wheel–rail interaction becomes more sensitive to these irregularities, resulting in higher peak L/V values. However, these peaks are predominantly transient and do not necessarily indicate a critical derailment condition.

As the speed increases to moderate levels (approximately 80–120 km/h), the vehicle exhibits improved dynamic stability, leading to a reduction in the L/V ratio. In this regime, the vehicle inertia helps attenuate the response to track irregularities, thereby reducing force fluctuations and resulting in lower derailment indices.

At higher speeds (e.g., 140 km/h), the L/V ratio increases again. This rise is primarily governed by the increase in centrifugal forces ($\propto v^2/R$), which enhances lateral wheel–rail interaction. Consequently, the lateral force increases more rapidly than the vertical load, leading to a higher L/V ratio and a greater propensity toward derailment. Overall, the results indicate that derailment risk is influenced by a combination of track irregularities at lower speeds and centrifugal effects at higher speeds, with an intermediate speed range exhibiting relatively safer operating conditions.

3.3 Effect of Curvature

The variation of the derailment coefficient (L/V ratio) along the track length for different curve radii at 100 km/h is shown in Fig. 7. In the initial straight section (up to 50 m), the L/V ratio remains negligible for all cases. A sharp increase is observed in the transition region (50–100 m) due to the gradual introduction of curvature and cant, which enhances lateral wheel–rail forces.

In the curved region, the L/V ratio exhibits oscillatory behaviour due to track irregularities; however, a clear dependence on curve radius is evident. The smallest radius ($R = 250$ m) yields the highest L/V values, while larger radii ($R = 320$ m and $R = 500$ m) show progressively lower levels. This trend is consistent with the centrifugal effect ($\propto v^2/R$), where tighter curves generate higher lateral forces and, consequently, higher derailment coefficients.

The maximum L/V value is approximately 0.5, observed at the leading (front) wheelset, and remains below the Nadal limit, indicating safe operation under the given conditions.

3.4 Influence of Track Irregularities

The influence of track irregularities on the derailment coefficient (L/V ratio) was examined by scaling their amplitude at a constant speed of 100 km/h, as shown in Fig. 8. Four cases were considered: a smooth track, baseline irregularities, and scaled irregularities of $0.5\times$ and $1.5\times$.

In the straight region , the L/V ratio remains negligible for all cases. A sharp increase is observed in the transition region due to the introduction of curvature and cant. Beyond this region, the L/V response exhibits oscillatory behaviour driven by track irregularities.

Although an increase in irregularity amplitude leads to slightly higher peak fluctuations (notably for the $1.5\times$ case), the overall L/V levels remain closely grouped across all cases. In particular, the $0.5\times$ and $1.0\times$ cases show nearly identical responses, indicating a relatively weak sensitivity of the derailment coefficient to moderate changes in irregularity amplitude under the given operating conditions.

The maximum L/V value is approximately 0.52, observed at the leading wheelset, and remains below the Nadal limit, confirming safe operation at 100 km/h.

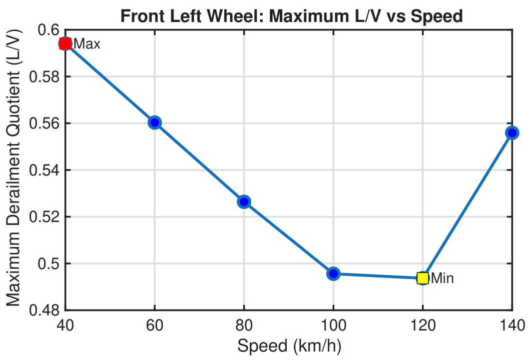

Figure 5: L/V vs Speed of Front Left Wheel

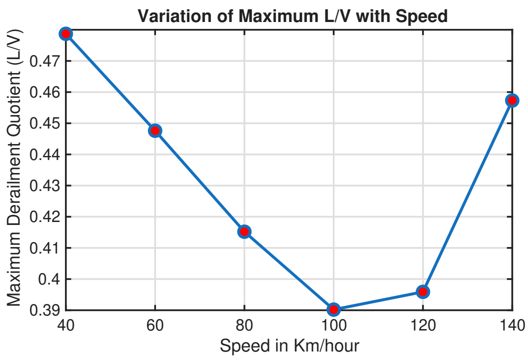

Figure 6: L/V vs Speed of Rear left wheel

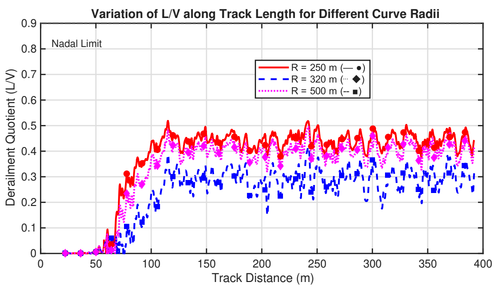

Figure 7: L/V vs Curvature

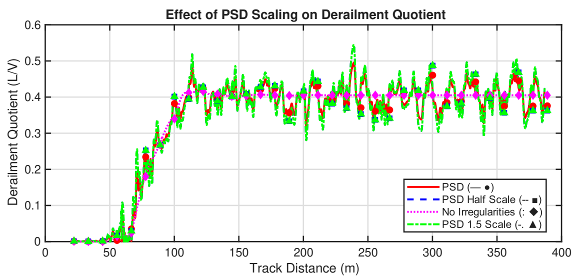

Figure 8: L/V vs Irregularities Amplitude

3.5 Critical Condition

Based on the fixed-parameter analysis, 140 km/h was identified as a near-critical operating speed. Accordingly, a detailed investigation was carried out at this speed for different curve radii and irregularity scaling, as shown in Fig. 9. For the sharp curve ($R = 250$ m), the derailment coefficient exhibits a sudden and extremely large spike in the front wheel (Fig. 9a), significantly exceeding the Nadal limit. This behaviour indicates loss of stable wheel–rail contact and represents a dynamically unstable condition rather than a physically sustained force level. A similar trend is observed in the rear wheel (Fig. 9b), where the L/V ratio exceeds the safety limit and subsequently drops, suggesting intermittent loss of contact. For the intermediate radius ($R = 320$ m), the L/V ratio approaches and intermittently exceeds the Nadal limit, particularly under amplified irregularities. This indicates a marginally unstable operating condition, where derailment risk is highly sensitive to track excitation.

In contrast, for the larger radius ($R = 500$ m), the L/V ratio remains well below the Nadal limit for both front and rear wheelsets, with values around 0.4–0.5. The response is comparatively stable, indicating safe operation even at 140 km/h.

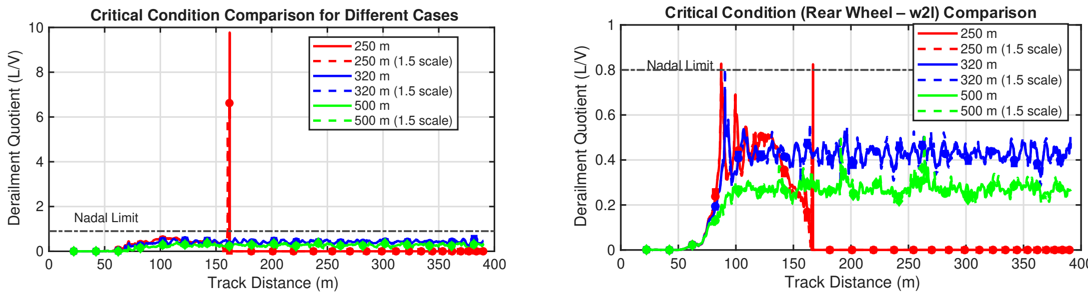

(a) Front Left Wheel

(b) Rear Left Wheel

Figure 9: Critical condition comparison of front and rear wheelsets

Overall, the results demonstrate that derailment behaviour at high speeds is strongly governed by curve radius. While sharp curves lead to instability and potential loss of contact, larger radii maintain stable wheel–rail interaction. Irregularity scaling further amplifies the response but does not alter the fundamental stability trend dictated by curvature.

3.6 Assessment of Derailment Risk

The derailment risk is evaluated using the L/V ratio based on the Nadal criterion, together with wheel unloading behaviour. The results show that derailment susceptibility is governed by the combined effects of vehicle speed, track curvature, and irregularity-induced excitation.

At moderate speeds (up to $\sim$100 km/h), the L/V ratio remains well below the Nadal limit for all cases, indicating stable wheel–rail contact. In this regime, irregularities mainly cause localized fluctuations without significantly affecting overall safety.

With increasing speed, the L/V ratio rises due to higher lateral forces and progressive wheel unloading. At 140 km/h, a transition in behaviour is observed. For $R = 250$ m, very large L/V spikes occur due to near-zero vertical load, indicating incipient loss of contact and dynamic instability rather than physically sustained forces. For $R = 320$ m, the L/V ratio approaches and intermittently exceeds the safety limit, representing a marginally stable condition sensitive to irregularities. In contrast, for $R = 500$ m, the L/V ratio remains below the threshold, indicating stable operation.

Irregularity scaling primarily affects fluctuation amplitude without significantly altering the mean L/V level, highlighting the dominant role of track geometry. Overall, three regimes are identified: (i) safe (low speed, large radius), (ii) marginal (high speed, moderate radius), and (iii) unstable (high speed, sharp curves with wheel unloading).

3.7 Asymmetric Wheel–Rail Interaction and Its Implications

The results clearly demonstrate pronounced asymmetric wheel–rail interaction between the left and right wheels, particularly in curved and transition regions. This asymmetry arises due to the combined effects of centrifugal force, cant, and geometric variation, which induce unequal load distribution across the wheelsets.

The outer rail (left wheel in the present configuration) experiences higher lateral forces and increased vertical loading, while the inner rail undergoes significant unloading. This effect becomes more pronounced with increasing speed, leading to a higher L/V ratio on the outer wheel and reduced vertical force on the inner wheel.

Furthermore, the front wheelset exhibits stronger asymmetric behaviour compared to the rear wheelset, as it directly encounters the transition geometry and irregularity inputs. The rear wheelset response is comparatively moderated due to dynamic filtering through the vehicle body and suspension system.

This asymmetric force distribution plays a critical role in derailment behaviour. Increased lateral loading on one side combined with unloading on the opposite side leads to elevated derailment coefficients and potential loss of contact. The results therefore highlight that derailment risk is inherently asymmetric and cannot be accurately assessed using symmetric assumptions.

Overall, the findings emphasize that asymmetric wheel–rail interaction, governed by the combined influence of speed, curvature, and irregularities, is a key mechanism driving instability in curved tracks.

4 Conclusion

This study investigated asymmetric wheel–rail interaction and derailment risk in curved railway tracks with transition geometry considering PSD-based track irregularities using a multibody dynamic simulation framework. The results indicate that the transition region (approximately 50–100 m) is a dynamically sensitive zone where the L/V ratio increases rapidly due to the progressive introduction of curvature and cant, while the circular section exhibits oscillatory behaviour governed by PSD-based irregularities.

A non-monotonic speed dependence of the L/V ratio is observed, decreasing from approximately 0.58 at 40 km/h to about 0.49 at 100–120 km/h, before increasing to nearly 0.55 at 140 km/h due to centrifugal effects and wheel unloading. Track curvature significantly affects derailment behaviour, with sharp curves ($R = 250$ m) producing higher L/V values, whereas larger radii ($R = 320$ m and $R = 500$ m) maintain comparatively stable responses. At higher speeds, particularly 140 km/h, larger force oscillations and pronounced asymmetric wheel–rail interaction increase derailment susceptibility, especially for smaller radii.

Overall, derailment risk is governed by the coupled influence of speed, track geometry, and PSD-based irregularities, with vehicle speed and curve radius having the strongest effect on wheel–rail stability.

Future work may extend the developed framework by incorporating wheel and rail wear, variable friction conditions, traction and braking forces, and localized track defects. The methodology can also be applied to different vehicle types and validated using experimental or field measurements to enhance its practical applicability.

Acknowledgements

References

[1] J.J. Kalker, "Three-Dimensional Elastic Bodies in Rolling Contact", Kluwer Academic Publishers, 1990.

[2] S. Iwnicki (Ed.), "Handbook of Railway Vehicle Dynamics", Taylor & Francis, 2006.

[3] R. Garg, R.V. Dukkipati, "Dynamics of Railway Vehicle Systems", Academic Press, San Diego, USA, 1984.

[4] O. Polach, "Creep Forces in Simulations of Traction Vehicles Running on Adhesion Limit", Wear, 258, 992–1000, 2005.

[5] O. Polach, "Influence of Wheel/Rail Contact Geometry on the Behaviour of a Railway Vehicle at Stability Limit", Proceedings of ENOC-2005, Eindhoven, Netherlands, 2005.

[6] S.L. Grassie, R.W. Gregory, K.L. Johnson, "The Dynamic Response of Railway Track to High Frequency Longitudinal Excitation", Journal of Mechanical Engineering Science, 24(2), 97–109, 1982.

[7] J. Pombo, J. Ambrósio, "A Computational Efficient General Wheel–Rail Contact Detection Method", Journal of Mechanical Science and Technology, 19(1), 411–421, 2005.

[8] J. Pombo, J. Ambrósio, "An Alternative Method to Include Track Irregularities in Railway Vehicle Dynamic Analyses", Nonlinear Dynamics, 68, 161–176, 2012.

[9] X. Lei, N.-A. Noda, "Analyses of Dynamic Response of Vehicle and Track Coupling System with Random Irregularity of Track Vertical Profile", Journal of

Sound and Vibration, 258(1), 147–165, 2002.
[10] K. Zboiński, "Dynamical Investigation of Railway Vehicles on a Curved Track", European Journal of Mechanics - A/Solids, 17, 1001–1020, 1998.
[11] Y.Q. Sun, M. Dhanasekar, "A Dynamic Model for the Vertical Interaction of the Rail Track and Wagon System", International Journal of Solids and Structures, 39, 1337–1359, 2002.
[12] P. Gorai, S.K. Saha, R.K. K., S. Panda, B. Manna, "Rail Vehicle-Track Interaction in Bridge Transition Zone using Multibody-Dynamic Approach", Proceedings of the Sixth International Conference on Railway Technology: Research, Development and Maintenance, Civil-Comp Conferences, Vol. 7, Paper 17.3, 2024.
[13] A. Matsumoto, Y. Sato, H. Ohno, M. Shimizu, J. Kurihara, M. Tomeoka, T. Saitou, Y. Michitsuji, M. Tanimoto, Y. Sato, M. Mizuno, "Continuous Observation of Wheel/Rail Contact Forces in Curved Track and Theoretical Considerations", Vehicle System Dynamics, 50(Suppl. 1), 349–364, 2012.
[14] S.K. Sharma, A. Kumar, R.C. Sharma, "Challenges in Railway Vehicle Modeling and Simulations", (ICNDME-2014), 453–462, 2014.
[15] X. Jin, Z. Wen, K. Wang, X. Xiao, "Effect of Passenger Car Curving on Rail Corrugation at a Curved Track", Wear, 260, 619–633, 2006.
[16] V. Kumar, V. Rastogi, P.M. Pathak, "Modelling and Evaluation of the Hunting Behaviour of a High-Speed Railway Vehicle on Curved Track", Proceedings of the Institution of Mechanical Engineers, Part F: Journal of Rail and Rapid Transit, 233(2), 220–236, 2019.
[17] S. Vishnu, S. Garg, S.P. Singh, S.K. Saha, "Differential Parameterization of Rail Vehicle Properties and Its Impact on Hunting", Proceedings of the Institution of Mechanical Engineers, Part F: Journal of Rail and Rapid Transit, 238, 48–58, 2024.
[18] C. Uyulan, M. Gokasan, S. Bogosyan, "Hunting Stability and Derailment Analysis of the High-Speed Railway Vehicle Moving on Curved Tracks", International Journal of Heavy Vehicle Systems, 26(6), 824–853, 2019.
[19] W. Zhai, "Vehicle–Track Coupled Dynamics: Theory and Applications", Springer, 2020.
[20] Y.Q. Sun, "Mitigating Train Derailments Due to Sharp Curve and Overspeed", Frontiers in Mechanical Engineering, 4, 8, 2018.
[21] S. Iwnicki, "Manchester Benchmarks for Rail Vehicle Simulation", Vehicle System Dynamics, 30, 295–313, 1998.
[22] G. Perrin, C. Soize, D. Duhamel, C. Funfschilling, "Track Irregularities Stochastic Modeling", Probabilistic Engineering Mechanics, 34, 123–130, 2013.
[23] H. Weinstock, "Wheel Climb Derailment Criteria for Evaluation of Rail Vehicle Safety", ASME Winter Annual Meeting, Paper No. 84-WA/RT-1, 1984.